

## Supporting Information

### Switching microobjects from low to high aspect ratios by a shape-memory effect

Fabian Friess<sup>a,b</sup>, Andreas Lendlein<sup>a,b,\*</sup>, and Christian Wischke<sup>a,\*,#</sup>

<sup>a</sup> Institute of Active Polymers and Berlin-Brandenburg Center for Regenerative Therapies, Helmholtz-Zentrum Hereon, Kantstr. 55, 14513 Teltow, Germany

<sup>b</sup> Institute of Chemistry, University of Potsdam, Karl-Liebknecht-Str. 25, 14476 Potsdam, Germany

\* Correspondence: [Andreas.lendlein@hereon.de](mailto:Andreas.lendlein@hereon.de), [christian.wischke@pharmazie.uni-halle.de](mailto:christian.wischke@pharmazie.uni-halle.de)

# Current address: Institute of Pharmacy, Martin-Luther-University Halle-Wittenberg

## 1. Supporting detailed description of experimental methodologies

### 1.1 Preparation and thermomechanical characterization of pure PVA films

Solutions of PVA (Mowiol 3-85 or Mowiol 4-88, 18 g) in pure water (60 mL, 23 wt%) were pipetted (1.3 mL) into rectangular molds on a glass plate, which were built to a size of 5 cm x 1.2 cm by using self-gluing Teflon stripes (height = 0.3 mm) as casting frames. After 24 hours at room conditions, the water was evaporated and stable PVA-films could be detached from the glass plate. The films were subjected to further drying for 4 hours at 60 °C resulting in specimens with dimensions of 4.75 cm x 1.14 cm, which were relatively brittle at room temperature.

The thermal properties of PVA were evaluated by differential scanning calorimetry (DSC; DSC 204 F1, Netzsch) from the second heating cycle performed between 10 and 250 °C in nitrogen atmosphere with heating and cooling rates of 10 K·min<sup>-1</sup>.

Films were preheated to the programming temperature ( $T_{\text{prog}}$ ) inside of a thermo-chamber (BW91250, Zwick/Roell) of a tensile tester (Z005, Zwick/Roell) to become more flexible before insertion into the self-tightening testing clamps (pincer grips, 8122, 500 N, Zwick/Roell) in a fixed starting position ( $L_{x1} = 3.0$  cm). Sample deformations in the tensile tester were performed at 30 mm·min<sup>-1</sup> with a preforce of 1 N. After the maximum elongation was reached (e.g.,  $\varepsilon_{\text{ph}} = 150\%$ ), samples were cooled to room temperature.

The quantitative analysis of the shape-memory effect (SME) of PVA was based on the sample elongations  $\varepsilon$  considering the following four points during the programming/recovery cycles (Supporting Figure S1): ( $\varepsilon_1$ ) stress free, non-programmed samples; ( $\varepsilon_2$ ) programmed samples under stress at the desired, predefined phantom elongation  $\varepsilon_{\text{ph}}$ , ( $\varepsilon_3$ ) programmed samples under stress-free condition after fixation of temporary shape, and ( $\varepsilon_4$ ) samples after shape-recovery. Therefore, the total sample length before ( $L_1$ ) and after programming ( $L_3$ ) as well as the total sample length after temperature-induced shape recovery ( $L_4$ ) were measured under stress free conditions. Additionally, the clamped sample distance in the tensile tester (denoted as  $L_x$ ) before deformation ( $L_{x1}$ ) was used to determine the length of the exposed sample part after programming and shape fixation [ $L_{x3} = L_3 - (L_1 - L_{x1})$ ] and the length of the corresponding sample part after shape-recovery [ $L_{x4} = L_4 - (L_1 - L_{x1})$ ]. The shape-fixity rate  $R_f$  and shape-recovery rate  $R_r$  were calculated according to supplementary equation S1 and S2.

$$R_f = \left( \frac{\varepsilon_3}{\varepsilon_2} \right) \cdot 100\% = \left( \frac{\left( \frac{L_{x3}}{L_{x1}} - 1 \right) \cdot 100\%}{\varepsilon_2} \right) \cdot 100\% \quad \text{Equation S1}$$

$$R_r = \left( \frac{\varepsilon_2 - \varepsilon_4}{\varepsilon_2 - \varepsilon_1} \right) \cdot 100\% = \left( \frac{\varepsilon_2 - \left( \frac{L_{x4}}{L_{x1}} - 1 \right) \cdot 100\%}{\varepsilon_2 - 0} \right) \cdot 100\% \quad \text{Equation S2}$$

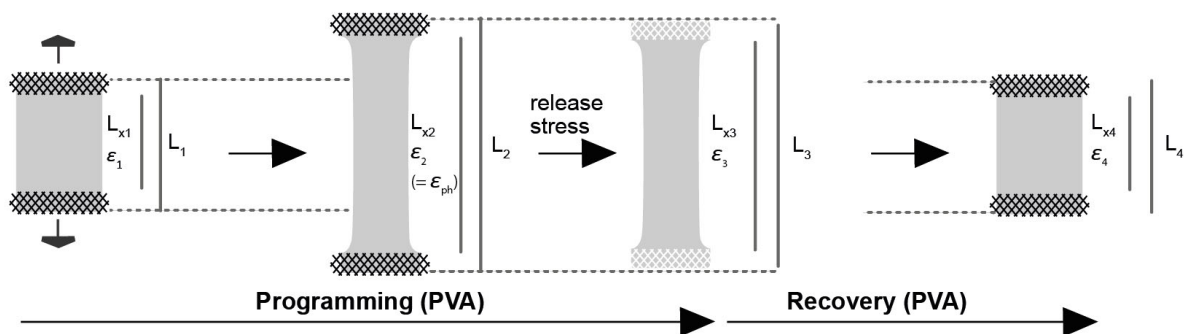


**Figure S1:** Schematic presentation of sample lengths and elongations during the quantitative evaluation of the shape-memory properties of PVA.

## 1.2 Synthesis and characterization of oCL-IEMA

Precursors for polymer micronetworks (<sup>2</sup>oCL-IEMA) were synthesized by nucleophilic addition, as established in literature (Macromol. Mater. Eng. 297: 1184-1192, 2012), of the two hydroxyl endgroups of linear oligo( $\epsilon$ -caprolactone) [<sup>2</sup>oCL-OH, 8 kDa, Perstorp, UK, 100 g, 12.5 mmol] to 2-isocyanatoethyl methacrylate (IEMA, 5.82 g, 5.30 mL, 37.5 mmol). The reaction was performed with personal safety equipment in a fume hood in dry argon atmosphere in 1 L dichloromethane (DCM) at 40 °C with addition of dibutyltin dilaurate (DBTL, 23.7 mg, 22.14  $\mu$ L, 37.5  $\mu$ mol) and stirring for 7 days. The reaction mixture was precipitated and washed with a mixture (8 L) of hexane, methanol and diethyl ether (Vol: 18/1/1), followed by filtration and drying at 35 °C in vacuum. The degree of functionalization ( $D_{a,NMR}$ ) of 99% was determined by <sup>1</sup>H-NMR spectroscopy in deuterated chloroform (Avance 500, Bruker). The

number-average molecular weight  $M_n$  of  $8000 \text{ g}\cdot\text{mol}^{-1}$  and a narrow polydispersity (PD) of 1.5 was confirmed by gel permeation chromatography in chloroform (GPC;  $35 \text{ }^\circ\text{C}$ ;  $1 \text{ ml}\cdot\text{min}^{-1}$ ; SDV linear M columns, PSS GmbH) based on a universal calibration with refractive index (Shodex RI-101, Showa Denko) and viscosity detectors (T60A, Viscotek Corp.).

### 1.3 Microfluidic templating of precursor microparticles

Microparticles from precursor ( $^2\text{oCL-IEMA}$ ) were prepared by an emulsification-based templating technique in a 2-needle glass capillary microfluidic device in the dripping regime (Int. J. Pharm. 567: 118461, 2019). A solution of the  $^2\text{oCL-IEMA}$  in a solvent mixture from ethyl acetate (EA) and dichloromethane (DCM) formed the o-phase [625 mg in 11.875 mL (EA:DCM, 1:1 v/v);  $\rho = 1.11 \text{ g}\cdot\text{mL}^{-1}$  at  $20^\circ\text{C}$  (DMA 4500, Anton Paar);  $w_{\text{oCL}} = 4.53 \text{ wt.}\%$ ]. The aqueous, continuous phase (w) consisted of 2.5 wt.% of PVA (Mowiol 4-88, 10 g) dissolved in pure water (390 mL). The three inlets of the 2-needle glass-capillary device were connected to a pressure-controlled pumping system, which was externally supplied with compressed air and equipped with calibrated flow sensors (Pressure controller: OB1, Elveflow;  $p_{\text{max}} = 2 \text{ bar}$ , flow sensors: (org)  $q_{\text{max}} = 80 \text{ }\mu\text{L}\cdot\text{min}^{-1}$ , (aq)  $q_{\text{max}} = 1 \text{ ml}\cdot\text{min}^{-1}$ ). This microfluidic device was operated with the o-phase as dispersed phase and two streams of w-phase as continuous phase to form the oil-in-water emulsion. The calibrated flow rates ( $q$ ) were set to  $0.75/5/5 \text{ mL}\cdot\text{h}^{-1}$  (o/w/w).

After continuous droplet production for 10 hours, the emulsion was stirred for another 5 hours to extract and evaporate the solvent and obtain hardened, semi-crystalline particles. To remove gas inclusions from the microparticles, the suspension was briefly exposed to  $70 \text{ }^\circ\text{C}$  for 1 min under gentle agitation by an overhead stirrer followed by cooling to RT. The size and size distribution of microparticles were determined before and after heating by static light scattering

confirming a narrow size distribution (Fraunhofer model, multiple narrow modes, Mastersizer 2000, Malvern). The microparticle suspensions were up-concentrated by centrifugation (3000 rpm, Biofuge) in 50 mL tubes and washed with water on a filter (0.45  $\mu\text{m}$ , NL17, Whatman<sup>®</sup>) until bubble formation stopped, suggesting removal of excess PVA. Subsequently, the precursor microparticles were collected from the filter, frozen in liquid nitrogen and lyophilized.

In this approach, the emulsification procedure had an approximated production frequency ( $f$ ) of 3800 droplets $\cdot\text{s}^{-1}$  ( $f = q \cdot V_{\text{drop,calc}}^{-1}$ ). This value is based on the assumption that the mass fraction of precursor  $w_{\text{oCL}}$  in the organic phase roughly equals the volume ratio  $\Phi_{\text{oCL}}$  of precursor in this solution. Accordingly, the droplet volume ( $V_{\text{drop,calc}} = V_{\text{MP,calc}} \cdot \Phi_{\text{oCL}}^{-1} = 0.055 \text{ nl}$ ) and the droplet diameter ( $d_{\text{drop,calc}} = (6 \cdot V_{\text{drop,calc}} \cdot \pi^{-1})^{1/3} = 47 \mu\text{m}$ ) were calculated from the average diameter ( $d_{\text{MP}} = 16.8 \mu\text{m}$ , D[4.3], volume-moment mean diameter) of semi-crystalline MPs.

#### 1.4 Particle embedding, MN crosslinking and programming in PVA phantoms

The embedding of precursor particles in PVA films has been reported before and adapted here (Polym Commun 30: 130-132, 1989; Langmuir 30: 2820-2827, 2014). Precursor particles were embedded in PVA films using a suspension of particles in 23 wt.% aqueous PVA (Mowiol 3-85) solution (200 mg particles in 13 mL, 1.5% [m/v]). The molds (6.8 cm x 2.3 cm) hosted a total volume of 3.7 mL. First, 1.1 mL of pure 23 wt.% PVA-solution were evenly distributed at both narrow edges of the mold, then 1.5 mL of precursor particles suspension were added in the center of the mold, followed by adding another 1.1 mL PVA-solution evenly distributed at the narrow mold edges (Figure S4A). After drying first at room temperature for 24 h (Figure S4B) and then at 60 °C for 4 h, the final particle loaded phantoms were obtained (6.4 cm x 2.2 cm). In this way, the precursor particles could be concentrated in the core part of the

phantom (Figure S4C), which was subjected to elongation and UV-irradiation later, thus avoiding to waste particles in the edges that were used to clamp the sample in the tensile tester.

For crosslinking of the molten precursor, free-radical polymerization was induced by UV-irradiation from an Omnicure-lamp (200 W high-pressure mercury lamp, Omnicure Series 2000, Internal Filter: 250-450 nm, IGB-Tech, Germany), which was equipped with a single-pole light guide (EXFO 806-00011, with a collimating adapter, IGB-Tech, Germany). The spherical light-spot with a diameter of 10 cm at the sample distance of 16 cm was centered at the sample center (Figure S4F). The light intensity at the sample was determined to be  $I = 80 \text{ mW}\cdot\text{cm}^{-2}$  (Plus+, A-40-D25-BBF, Laser Point). Skin and eye exposure to UV irradiation was prevented by personal safety equipment and coverage of the UV light path.

The following steps were conducted for programming:

- (i) PVA phantoms containing precursor microparticles were preheated to the programming temperature ( $T_{\text{prog}} = 65 \text{ }^{\circ}\text{C}$ ) inside the preheated tensile tester. Then, samples were inserted into self-tightening testing clamps placed in a fixed starting position ( $L_{x1} = 4.7 \text{ cm}$ ).
- (ii) For SME: Crosslinking inside the molten precursor droplets was induced by UV-irradiation for 20, 40 or 60 min. The irradiation was conducted at a sample distance of 16 cm (Figure S4F) with the light spot being adjusted to the sample center.  
For aSME: The phantoms were programmed at  $30 \text{ mm}\cdot\text{min}^{-1}$  with a preforce of 1 N to an elongation  $\varepsilon_{\text{ph}} = 150\%$  ( $T_{\text{prog PVA}} = 65 \text{ }^{\circ}\text{C}$ ) (Figure S3E). The molten, non-crosslinked precursor droplets adapted an ellipsoidal shape inside the phantoms.
- (iii) For SME: The phantom stretching (= micronetwork programming) was performed at  $30 \text{ mm}\cdot\text{min}^{-1}$  with a preforce of 1 N to an elongation of  $\varepsilon_{\text{ph}} = 150\%$ .

For aSME: Crosslinking of precursor droplets was performed inside the elongated phantoms at a sample distance of 16 cm (Figure S4F) with the light spot being adjusted to the sample center.

- (iv) The PVA phantoms were cooled in the thermo-chamber of the tensile tester to room temperature, allowing vitrification of the PVA phantoms and crystallization of the embedded crosslinked MN. The samples were removed from the clamps. At this step, SME MN are in their programmed temporary shape and aSME MN are in their non-programmed permanent shape.
- (v) Only for aSME: Samples were placed into a preheated oven to allow shape recovery of the phantom and simultaneous programming of the embedded and molten micronetworks towards lower longitudinal dimension ( $T_{\text{rec PVA}} = T_{\text{prog MN}} = 100 \text{ }^{\circ}\text{C}$ ). By removing the sample from the oven and cooling to room temperature, the programmed shape of the aSME micronetworks was fixed by PCL crystallization.
- (vi) Subsequently, the micronetworks were isolated by dissolving the PVA-matrix by addition of 30 mL of water and vortexing in 50 mL tubes. Finally, the programmed micronetworks were purified as described for microparticles.

## 1.5 Analysis of network formation and properties

The conversion of the precursor's methacrylate-endgroups (IEMA) upon UV-irradiation was determined from purified MN (powder) by IR-spectroscopy (Nicolet 6700, Thermo Scientific) with an ATR-unit (attenuated total reflectance) by analyzing the out of plane bending vibration of =CH<sub>2</sub> (815 cm<sup>-1</sup>).

The influence of network formation on the thermal properties of the purified PCL MN was evaluated by differential scanning calorimetry (DSC) from the second heating cycle performed between -100 and +150 °C in nitrogen atmosphere with heating and cooling rates of 10 K·min<sup>-1</sup>.

Furthermore, analysis by laser diffraction allowed the determination of the average diameter of swollen MN (Mastersizer 2000, Malvern), when the size measurement was performed in DCM instead of water. After exclusion of scattering artefacts, the main peak of the size distribution was included for calculation of the average diameter. This also allowed to determine a degree of swelling [ $Q = d_{MN,DCM}^3 \cdot (d_{MP,aq})^{-3}$ ] of 410±5% (SME-MN, 60 min UV). By applying the Flory-Rehner theory (according to equation S3) in respect of the polymer's volume fraction ( $\phi_2$ , equation S4), the polymer-solvent interaction parameter ( $\chi_{12} = -0.26$ ) of poly( $\epsilon$ -caprolactone) in DCM, the molar volume of the solvent  $V_1 = 63.8 \text{ ml}\cdot\text{mol}^{-1}$ , and the density of the polymer network  $\rho = 1.16 \text{ g}\cdot\text{ml}^{-1}$ , an average segment chain length ( $M_c$ ) between netpoints of 730±20 Da was estimated from the crosslink density of 1.60±0.05 mmol·ml<sup>-1</sup>.

$$v_c = \frac{\ln(1 - \phi_2) + \phi_2 + \phi_2^2 \chi_{12}}{V_1 [(\phi_2 / 2) - \phi_2^{1/3}]} = \frac{\rho}{M_c} \quad \text{Equation S3}$$

$$\phi_2 = \frac{V_{MN,aq}}{V_{MN,DCM}} \quad \text{Equation S4}$$

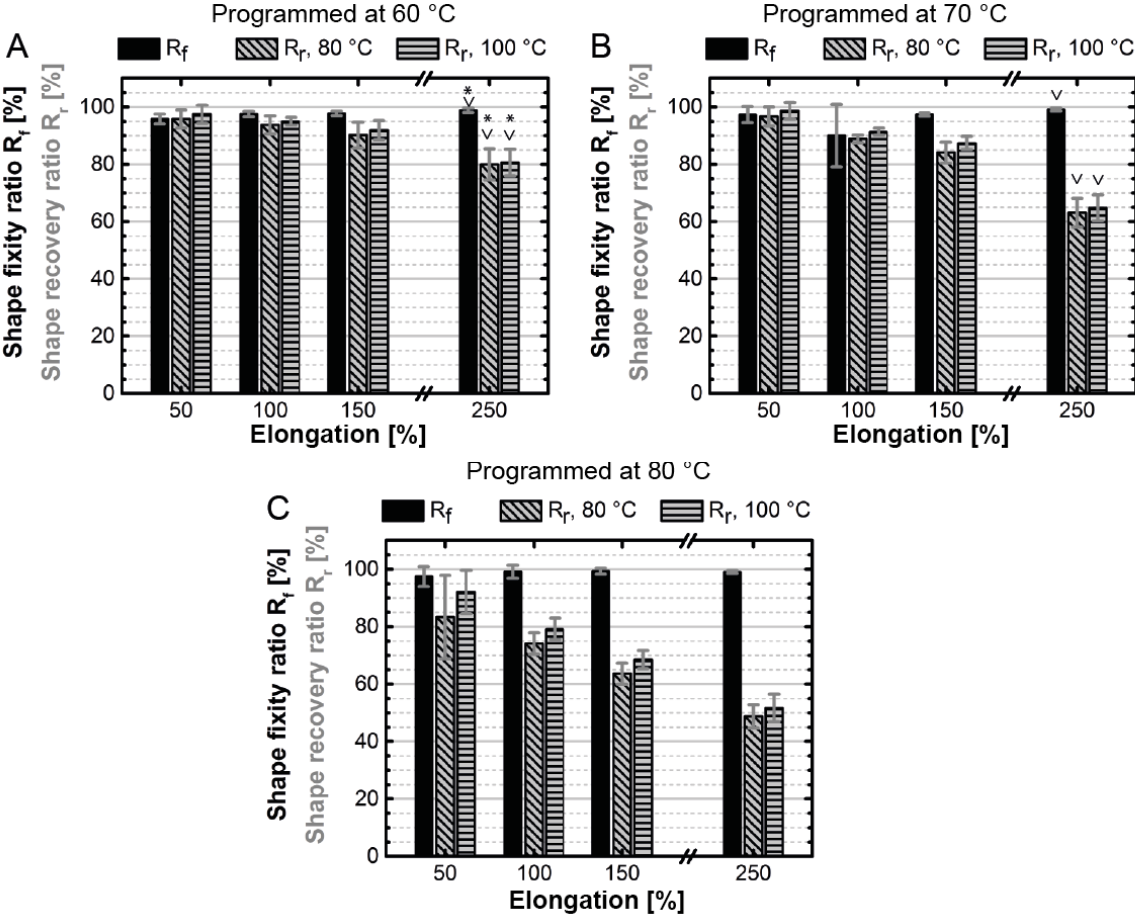
## 1.6 Analysis and quantification of shape-switching function

For microscopic monitoring (DMI 6000B, Leica) of solvent-induced shape switching, purified programmed MN were placed as suspension (pure water) on a microscopy slide. After water evaporation, the samples were covered with a glass cover slide. Under microscopic examination, approximately 40  $\mu\text{L}$  of dichlorormethane (DCM) was applied to swell the micronetworks, followed by DCM-evaporation and deswelling at room conditions.

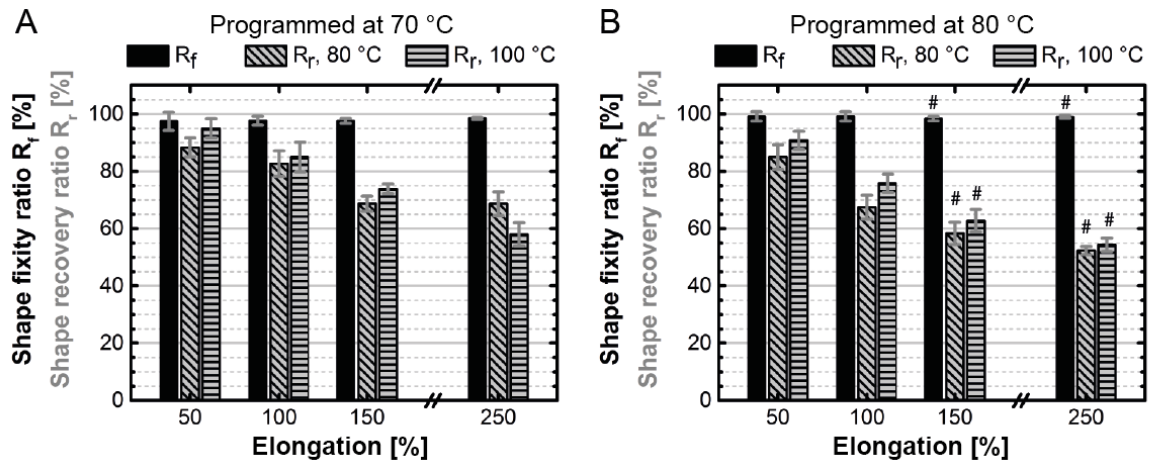


The temperature-induced shape-switching function of MN was monitored by light microscopy (Axio Imager.A1m, Carl Zeiss) in a closed heating chamber (LTS 350 stage chamber, Lincam), which was operated at heating and cooling rates of  $10 \text{ K}\cdot\text{min}^{-1}$ . Suspensions of programmed MN were placed on a microscopy slide. To reduce evaporation-driven convection, the suspension was covered with a thin glass slide and paraffin oil was applied along the edges for sealing. SME and aSME experiments were performed by heating from 35 to 70 °C with time-lapse imaging (1 image per 0.5 K). The images were evaluated with ImageJ particle analyzing tools (V1.46r, National Institute of Health, USA).

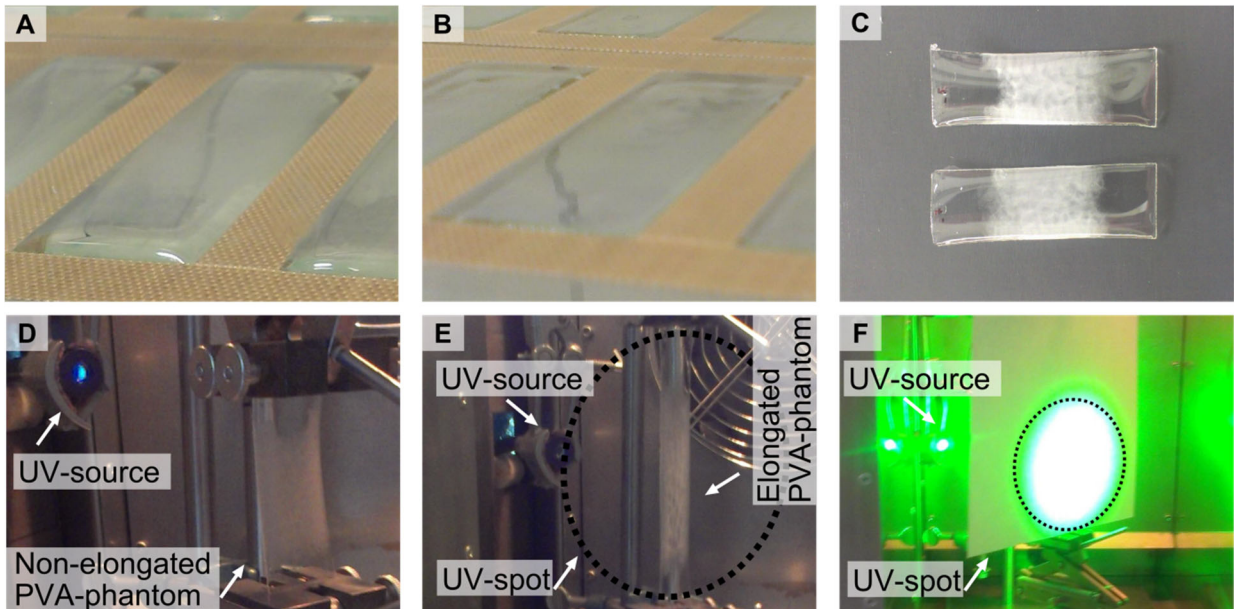
## 2. Supplementary Results



**Figure S2.** Characterization of the shape-memory effect of PVA 3-85 in thermomechanical tests with programming at (A) 60 °C, (B) 70 °C, and (C) 80 °C. The shape fixity ratio  $R_f$  as well as the shape recovery ratio  $R_r$  as determined after 1 h at 80 °C and 1 h at 100 °C are shown in dependence of the degree of elongation ( $\epsilon_{ph} = 50, 100, 150$  or 250%). (Mean, S.D.;  $n = 4-10$ , \*  $n = 3$ ; v high tendency to break)

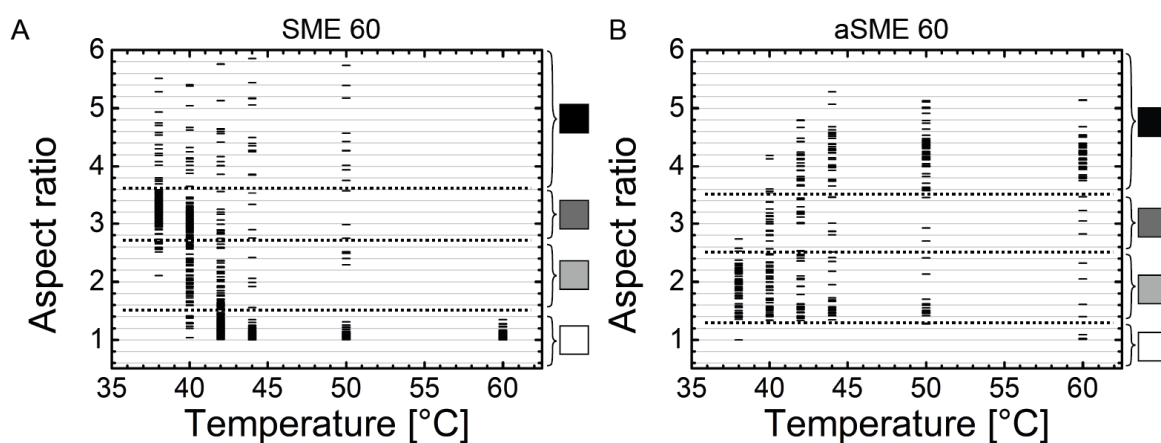


**Figure S3.** Characterization of the shape-memory effect of PVA 4-88 in thermomechanical tests with programming at (A) 70 °C and (B) 80 °C. The shape fixity ratio  $R_f$  as well as the shape recovery ratio  $R_r$  as determined after 1 h at 80 °C and 1 h at 100 °C are shown in dependence of the degree of phantom elongation ( $\varepsilon_{ph}$ ). (Mean, S.D.;  $n = 4-6$ ,  $^{\#}n = 2$ )

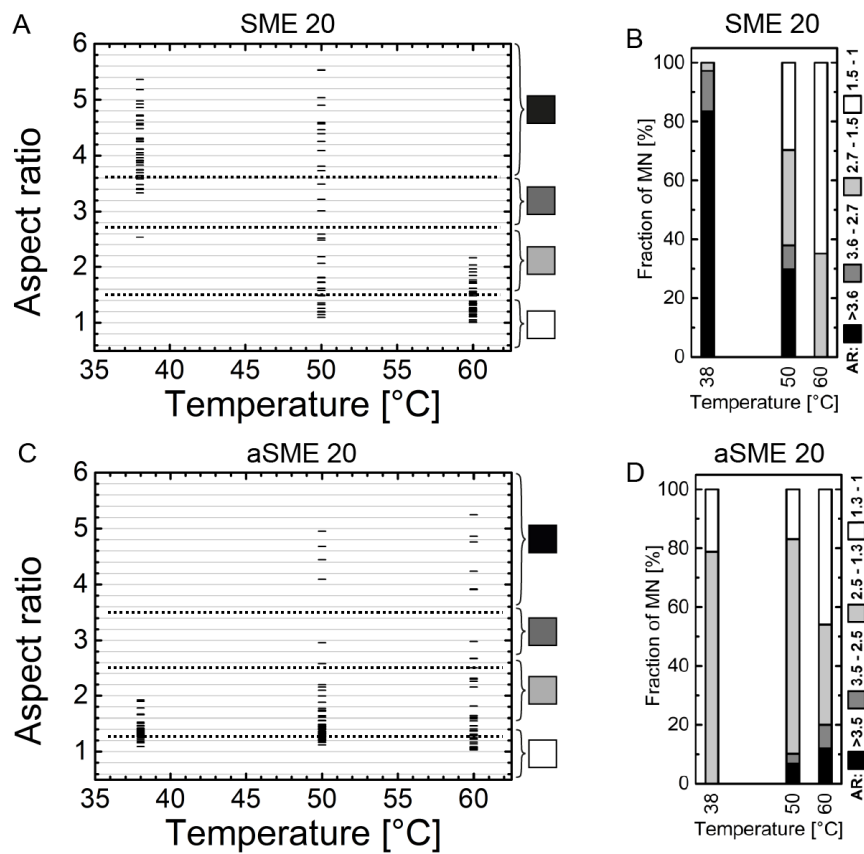


**Figure S4.** Setup and procedures to realized SME and aSME. (A-C) Phantom preparation as illustrated by (A) casted PVA solution in mold, (B) dried phantoms after 24 hours at ambient conditions, and (C) after subsequent drying at 60 °C for 4 h. (D-F)

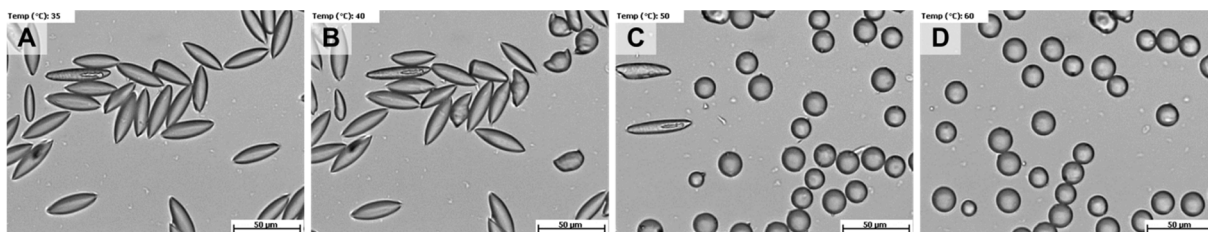
Instrumentation for crosslinking precursor MP to MN particles in PVA phantoms and thermomechanical treatment in tensile tester with UV source. (D: before elongation; E: after elongation and before UV light exposure; F: Visualization of position of the light spot with external green light interference filter [wavelength  $495 \text{ nm} > \lambda > 580 \text{ nm}$ ]). For crosslinking, the UV-irradiation was provided to the PVA phantom in a spherical spot of 10 cm diameter with a sample distance of 16 cm.



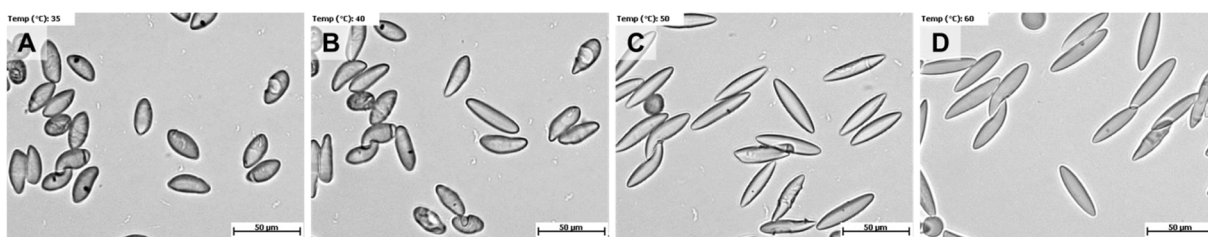
**Figure S5.** Aspect ratios of MN at different temperatures during the shape-recovery experiments for (A) SME60 and (B) aSME60. Dotted horizontal lines and colored squares indicate the size fractions, which are shown in the main manuscript (Fig. 5) as stacked column diagrams (SME:  $n = 195-258$ ; aSME:  $n = 51-64$ ). All micronetworks were synthesized by 60 min UV irradiation in phantoms.



**Figure S6.** Thermally-induced shape switching of MN, which were synthesized by irradiation for 20 min. Data for SME20 (A, B) and aSME20 (C, D), showing in (A,C) the AR of individual MN at different temperatures during heating (recovery) experiments and in (B,D) the data analysis in size fractions as defined by horizontal dotted lines in panel A and C. (SME20: n = 36-37; aSME20: n = 50-59).



**Suppl. Movie 1:** Images from a movie showing the temperature-induced shape-recovery of SME60 MN with a decrease of their  $AR$  at  $T_{sw}$ . Data for the temperature interval from 35 to 60 °C with a heating rate of 10 K·min<sup>-1</sup>. Images at (A) 35 °C, (B) 40 °C, (C) 50 °C, (D) 60 °C.



**Suppl. Movie 2:** Images from a movie showing the temperature-induced shape-recovery of aSME60 MN with an increase of their  $AR$  at  $T_{sw}$ . Data for the temperature interval from 35 to 60 °C with a heating rate of 10 K·min<sup>-1</sup>. Images at (A) 35 °C, (B) 40 °C, (C) 50 °C, (D) 60 °C.